

Direct Decomposition of NO into N₂ and O₂ on SrFe_{0.7}Mg_{0.3}O₃ Perovskite Oxide

Hideharu Iwakuni, Yusuke Shinmyou, Hiroshige Matsumoto, and Tatsumi Ishihara*

Department of Applied Chemistry, Faculty of Engineering, Kyushu University,
744 Motooka, Nishi-ku, Fukuoka 819-0395

Received April 27, 2007; E-mail: ishihara@cstf.kyushu-u.ac.jp

NO direct decomposition on doped SrFeO₃ perovskite oxide was investigated. The ability of SrFeO₃ for direct decomposition of NO is strongly affected by the dopant in Fe sites. Among the examined dopants and compositions, the highest yield of N₂ was achieved on SrFe_{0.7}Mg_{0.3}O₃. When SrFe_{0.7}Mg_{0.3}O₃ was loaded with Pt, the N₂ yield further improved, and the light-off temperature fell by 100 K. On this catalyst, the yields of N₂ and O₂ were 56 and 35%, respectively, at 1123 K. On the Pt-loaded SrFe_{0.7}Mg_{0.3}O₃ catalyst, the NO decomposition rate increased with increase in the NO partial pressure with $P_{\text{NO}}^{1.31}$. The presence of oxygen slightly decreased the N₂ yield with $P_{\text{O}_2}^{-0.12}$. Therefore, the effect of oxygen poisoning on NO decomposition upon Pt-loaded SrFe_{0.7}Mg_{0.3}O₃ is small. From the result of O₂-TPD, Pt loading possibly weakens the adsorption strength of surface oxygen and enhances NO adsorption. In summary, this study shows that the substitution of Fe with lower valence cation in SrFeO₃ and also loading a small amount of Pt are highly effective for increasing the NO decomposition activity.

Nitrogen oxides (NO_x), which mainly form in lean combustion engines, such as diesel engines, are extremely toxic to the human body and also harmful to environment, because they are one of the main sources of both acid rain and photochemical smog. At present, because of the increase in the number of the diesel engine cars, the amount of NO_x emission in urban area has increased significantly. Several methods have been proposed for NO_x removal.^{1–3} Among them, the selective reduction of NO_x by hydrocarbons has been studied extensively, and various catalysts,^{4–14} in particular, Cu-ZSM-5, have been proposed as an active catalyst for this reaction.^{15–19} However, due to the low selectivity of the reductant, this method is not practical. Instead of hydrocarbon reduction, selective reduction of NO_x with urea is now considered the most promising method for the removal of NO_x under oxygen containing atmosphere. However, for this method, a slight excess of urea to NO_x is required and so, environmental problems from urea or ammonia formed are also possible. On the other hand, direct decomposition of NO into N₂ and O₂ (2NO = N₂ + O₂) is the most ideal reaction for NO_x removal, because the process is quite simple.^{20,21} However, it is well known that the formed oxygen adsorbs strongly on the catalyst, resulting in the deactivation of the catalyst. Some catalysts, such as Cu-ZSM-5,²² Co-ZSM-5 (which contains Co in the framework²³), La₂O₃,²⁴ Ba/MgO,²⁵ and LaCoO₃²⁶ based perovskite oxides, are active toward the direct decomposition of NO. In particular, Teraoka et al. have reported that La_{0.8}Sr_{0.2}CoO₃ is highly active toward NO decomposition and that the N₂ yield is 40% at 1073 K.²⁷ Although the reaction temperature is higher, high NO decomposition activity is expected on perovskite oxides. High reaction temperatures are sometimes better from the viewpoint of practical applications, because the negative effects of oxygen, water, and sulfur compounds seem to decrease with an increase in the temperature.

In our previous study, NO direct decomposition over LaMnO₃ perovskite oxide doped with Ba for the La site and In for the Mn site has been investigated, and it has been found that La_{0.7}Ba_{0.3}Mn_{0.8}In_{0.2}O₃ perovskite oxide exhibits high activity toward NO direct decomposition over 1073 K.²⁸ On the other hand, NO direct decomposition with Fe⁴⁺, which is an anomalous valence number of Fe at high temperature, has hardly been studied. Shin et al. have reported that brownmillerite-like compound of Sr₂Fe₂O₅ exhibits rather high NO decomposition activity in the range of 973–1173 K.^{29–31} In addition, they have also shown that an oxygen-deficient perovskite of composition SrFeO_{3–x} selectively absorbs NO gas above approximately 373 K, and analysis of the infrared spectrum of the system ¹⁴NO–¹⁵NO–SrFeO_{3–x} has shown that the absorbed species in SrFeO_{3–x} is possibly the nitrosyl ion (NO[–]) bound to the iron ion accommodate in some oxygen vacancies.³² However, except for their IR study on NO adsorption species on SrFeO₃, the number of studies on the NO decomposition activity of oxides consisting of Fe^{IV} is limited. Perovskite oxide, which contains Fe⁴⁺, is expected to be a new NO direct decomposition catalyst, since reduction of Fe⁴⁺ to Fe³⁺ proceeds easily and the removal of the surface oxygen can be easily achieved at reasonably low temperature. In this study, effects of various dopants at the Fe site in SrFeO₃ on NO decomposition activity were investigated. NO decomposition activity was greatly improved by a small amount of dopant in case of LaMnO₃ or BaMnO₃ catalyst.

Experimental

Doped SrFeO₃ were prepared by a conventional solid-state reaction method. The precursor of SrFeO₃ was obtained by evaporating an aqueous solution of a calculated amount of Sr(NO₃)₂, Fe(NO₃)₃, and metal nitrates. The mixtures obtained were precalcined in air at 673 K for 2 h to decompose the metal nitrates,

Table 1. NO Direct Decomposition into N₂ and O₂ over SrFe_{0.7}M_{0.3}O₃

Catalyst	Specific surface area/m ² g ⁻¹	Conversion/%	Yield/%			
		NO	N ₂	O ₂	N ₂ O	NO ₂ ^{a)}
SrFe _{0.7} M _{0.3} O ₃						
M = Mg	1.7	86.4	47.3	23.4	0.0	31.5
Sn	0.8	79.1	42.7	19.0	0.0	30.1
Ni	1.2	76.1	41.6	17.2	0.0	29.5
Ce	1.3	77.7	41.3	14.2	0.0	31.8
Zr	1.6	78.1	37.5	11.8	0.0	33.2
Mn	0.7	62.4	27.0	5.2	0.0	28.6
Ga	0.9	60.1	25.5	4.3	0.0	27.9
Co	0.6	48.2	17.3	2.6	0.0	22.8
Ru	1.4	29.6	13.2	1.7	0.0	14.0
Ir	2.0	26.1	11.1	1.6	0.0	12.3
Si	0.6	11.1	3.8	0.5	0.0	5.3
Ge	0.9	6.8	3.9	0.4	0.0	3.2
Cu	0.8	18.6	3.3	0.9	0.0	8.8
Ti	0.6	3.9	0.8	0.4	0.0	1.8

a) Estimated based on material balance of nitrogen. NO = 1%, He balance, $W/F = 3.0 \text{ g s cm}^{-3}$, temperature: 1123 K.

and then calcined in air at 1473 K for 6 h. X-ray diffraction was performed on this sample using a Cu K α line, and the formation of perovskite phase was confirmed. This catalyst powder was pressed into disks, crushed and sieved into 16 to 32 meshes. Pt (1 wt %) was loaded on SrFe_{0.7}Mg_{0.3}O₃ by conventional impregnation with tetraammineplatinum(II) chloride, 1-hydrate (Pt(NH₃)₄Cl₂·H₂O).

Direct decomposition of NO was performed with a conventional fixed-bed gas-flow reactor with a quartz glass tube (12-mm diameter). Gaseous mixture of 1% NO diluted with He was fed to the catalyst bed for NO direct decomposition reactions. The catalyst (1 g) was always set in the reactor by using quartz wool (ca. 0.5 cm in catalyst height), and the feed rate of the reactant was fixed at $W/F = 3.0 \text{ g s cm}^{-3}$, where W and F are the catalyst weight and the gas flow rate, respectively. Reaction was performed at 773–1123 K, and N₂, O₂, and fed NO were analyzed with online gas chromatography with a 5A molecular sieve column. N₂O was analyzed using a Porapak-Q column with a thermal conductivity detector (TCD). Because NO₂ cannot be analyzed with gas chromatography, NO₂ formation rate was estimated by the amount of nitrogen and oxygen molar amounts before and after the catalyst bed, namely average of (NO conversion–N₂ yield) and (N₂ yield–O₂ yield) values. In this study, the activity of the catalyst toward NO decomposition is mainly discussed based on the N₂ yield. It is also noted that the formation of N₂O was not observed in this study. Effects of the coexistence of O₂ were measured by mixing 1–5% O₂ diluted with He with the reactant gas. In order to keep the total flow rate of 20 mL min⁻¹ constant, the feed rate of He was varied as a balance gas.

Temperature-programmed desorption (TPD) of NO and O₂ was performed to analyze the adsorption state of O₂ and NO. After evacuation of the catalyst at 773 K for 1 h, the catalyst was exposed to 101 kPa NO or O₂ for 1 h, followed by cooling to room temperature. After evacuation at room temperature for 30 min, the catalyst was heated at 10 K min⁻¹, and the desorbed gas was monitored by using a quadrupole mass spectrometer (ANELVA, AQR-100R).

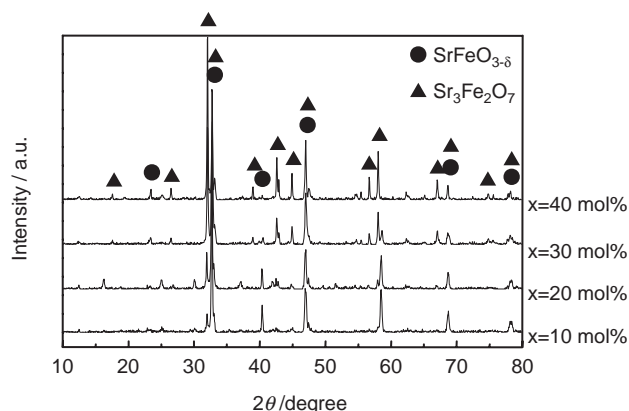
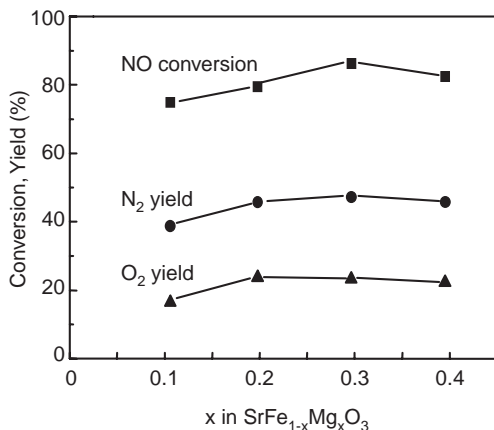
Adsorption state of NO was measured with FT-IR (JASCO type 610) with a diffuse reflection unit equipped with a heating unit and KBr window. The catalyst (ca. 0.15 g) was set into the measure-

ment pan and evacuated at 773 K for 3 h to remove the adsorbed water. After evacuation, a background spectrum was acquired at 773 K, and gaseous NO (ca. 10 kPa) was introduced into the measurement cell at 773 K. NO adsorption was performed at 773 K for 30 min, and the catalyst was cooled to room temperature. IR spectra of adsorbed NO were measured after evacuation of the catalyst at the described temperature for 30 min.

Results and Discussion

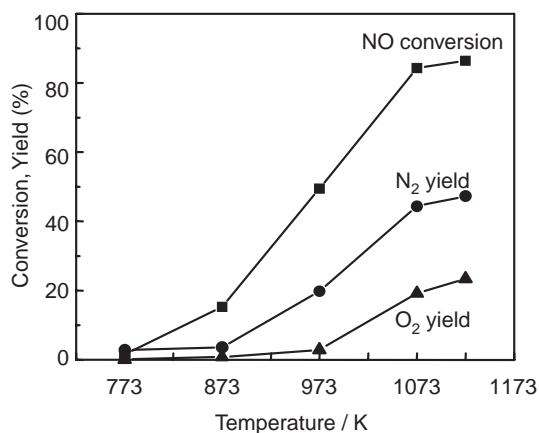
Effects of Dopant in SrFeO₃ on NO Direct Decomposition Activity. Table 1 shows the NO decomposition activities of SrFeO₃ perovskite oxide doped with various cations (Mg, Sn, Ni, Ce, Zr, Mn, Ga, Co, Ru, Ir, Si, Ge, Cu, and Ti). The NO direct decomposition activity of SrFeO₃ without dopant was not measured in this study, because it was not stable and its single phase cannot be obtained. Similar to LaMnO₃, the NO decomposition activity of the SrFeO₃ catalyst was strongly affected by additives. Among the catalysts examined, Mg-doped SrFeO₃ catalyst afforded the highest N₂ yield. Other catalysts, such as Sn, Ni, Ce, and Zr-doped catalysts, also exhibited fairly high N₂ formation rate. On the contrary, N₂ formation rates on Si, Ge, Cu, and Ti-doped catalysts were smaller than 4%. Therefore, doping with these cations, which are mainly tetravalent cations, does not enhance the NO decomposition activity. BET surface area of the doped SrFeO₃ is also shown in Table 1. Since BET surface area did not significantly change with the dopant, change in NO decomposition activity was assigned to the dopant effects. Since it was found that the Mg-dopant was the most effective for the direct decomposition of NO, Mg-doped SrFeO₃ was further studied in the following part.

Figure 1 shows the XRD patterns of SrFe_{1-x}Mg_xO₃ catalysts. The X-ray diffraction peaks shifted to a lower angle with an increase in the amount of Mg, suggesting an increase in the lattice constant. Considering the effective ionic radius of 6 coordination of Mg²⁺ is 86.0 pm, which is larger than that of 6-coordinate Fe⁴⁺ (72.5 pm) and that of 12-coordinate Sr²⁺

Fig. 1. XRD patterns of $\text{SrFe}_{1-x}\text{Mg}_x\text{O}_3$ prepared.Fig. 2. N_2 and O_2 yield on NO direct decomposition over $\text{SrFe}_{1-x}\text{Mg}_x\text{O}_3$ at 1123 K as a function of x value ($P_{\text{NO}} = 1\%$, $W/F = 3.0 \text{ g s cm}^{-3}$).

(158 pm),³³ it is thought that Mg replaces Fe, but not Sr, in SrFeO_3 . Although the formation of a small amount of $\text{Sr}_3\text{Fe}_2\text{O}_7$ phase was observed, the main diffraction peaks were assigned to those of SrFeO_3 . An impurity phase appeared when the x value was higher than 0.3 and became significant with an increase in the amount of Mg. Therefore, it seems likely that the solubility limit of Mg into Fe site of SrFeO_3 exists around $x = 0.3$ and Mg replaces Fe in SrFeO_3 lattice. Valence number of Fe in SrFeO_3 is +4 from the molecular formula, which is an unusual valence number, and by doping lower valence cations of Mg, the number of oxygen vacancies is increased for charge compensation. The Fe^{4+} ion is not stable at high temperatures, and so, the solid solubility of Mg into Fe site is not large due to the low lattice stability. In any case, at x values less than 0.3, the main phase of Mg-doped sample is a perovskite structure of SrFeO_3 .

Figure 2 shows the N_2 and O_2 yield on NO direct decomposition over $\text{SrFe}_{1-x}\text{Mg}_x\text{O}_3$ catalyst at 1123 K as a function of x value. It was observed that the N_2 yield as well as O_2 yield increased with an increase in the amount of Mg and the yields reached a maximum at $x = 0.3$, which is close to the solid solubility limit of Mg. After the N_2 and O_2 yield became saturated at ca. 47 and 23%, respectively, a further increase in the amount of Mg decreased the N_2 and O_2 yield. Considering the solubility limit of Mg, it is seen that the optimum

Fig. 3. Temperature dependence of NO decomposition activity upon $\text{SrFe}_{0.7}\text{Mg}_{0.3}\text{O}_3$ in the range of 773–1123 K ($P_{\text{NO}} = 1\%$, $W/F = 3.0 \text{ g s cm}^{-3}$).

amount of Mg into Fe site is at $x = 0.3$. As a result, the optimum amount for Mg doping is 30 mol % of Fe sites in SrFeO_3 .

Temperature dependence of NO decomposition activity upon $\text{SrFe}_{0.7}\text{Mg}_{0.3}\text{O}_3$ is shown in Fig. 3. It was observed that NO decomposition started around 873 K, at which N_2 and O_2 start to form. N_2 and O_2 yield monotonically increased with the reaction temperature. N_2 yield reached a value of 47% at 1123 K. Although the contact time is much longer and the NO concentration is much higher than that of the actual exhaust gas from engines, it was found that fairly high NO conversion could be achieved on $\text{SrFe}_{0.7}\text{Mg}_{0.3}\text{O}_3$ catalyst. Therefore, perovskite oxide of $\text{SrFe}_{0.7}\text{Mg}_{0.3}\text{O}_3$ is an interesting NO decomposition catalyst, although a high reaction temperature is required.

Effects of Pt Loading on $\text{SrFe}_{0.7}\text{O}_3$ on NO Direct Decomposition Activity. In order to improve the NO decomposition activity, loading a small amount of a precious metal is sometimes effective. For example, it has been reported that loading Pt on TiO_2 , SiO_2 , and Al_2O_3 is effective for increasing NO decomposition activity.³⁴ It has also been reported that Pt loading is effective for increasing the NO decomposition activity on a $\text{BaO}/\text{Al}_2\text{O}_3$ catalyst.³⁵ In this study, effects of 1 wt % Pt loading for $\text{SrFe}_{0.7}\text{Mg}_{0.3}\text{O}_3$ on the NO decomposition activity were also studied. Temperature dependence of NO decomposition activity upon Pt-loaded $\text{SrFe}_{0.7}\text{Mg}_{0.3}\text{O}_3$ is shown in Fig. 4. The NO decomposition activity improved greatly due to Pt-loading. In addition, the N_2 yield improved from 47 to 56%, and the O_2 yield increased from 23 to 36% at 1123 K by loading Pt. Therefore, it can be said that the loading Pt is quite effective for improving the NO decomposition activity of $\text{SrFe}_{0.7}\text{Mg}_{0.3}\text{O}_3$. At present, a detailed mechanism for the improved NO decomposition activity by Pt loading is not clear; however, loading Pt did not always improve the NO decomposition activity. In fact, loading Pt into BaMnO_3 simply decreased the NO decomposition activity. Therefore, improvement in NO decomposition activity is not a simple summation of the activity of Pt and SrFeO_3 catalyst. It is considered that there are synergy effects between Pt and $\text{SrFe}_{0.7}\text{Mg}_{0.3}\text{O}_3$. The light-off temperature of NO decomposition activity also shifted by as much as 100 K to a lower temperature. Effects of

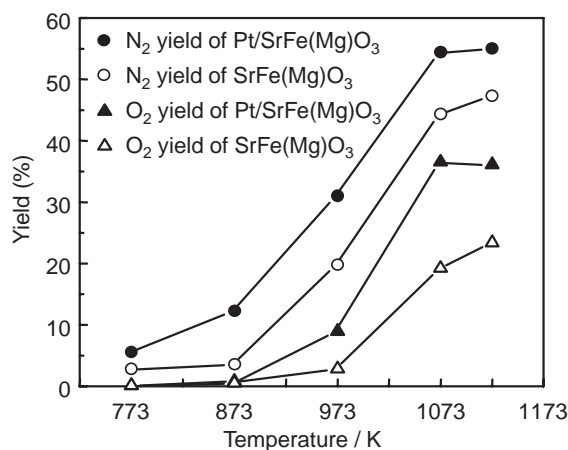


Fig. 4. Temperature dependence of NO decomposition activity upon 1 wt % Pt/SrFe_{0.7}Mg_{0.3}O₃ in the range of 773–1123 K ($P_{\text{NO}} = 1\%$, $W/F = 3.0 \text{ g s cm}^{-3}$).

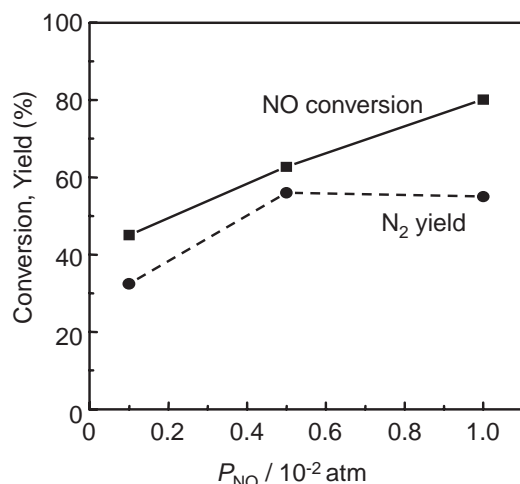


Fig. 5. NO conversion and N₂ yield from NO direct decomposition over 1 wt % Pt/SrFe_{0.7}Mg_{0.3}O₃ as a function of NO partial pressure at 1123 K ($W/F = 3.0 \text{ g s cm}^{-3}$).

reaction conditions on NO decomposition activity are also reported.

Figure 5 shows the N₂ formation rate as a function of NO partial pressure. From our previous study, the N₂ formation rate increases with an increase in the NO partial pressure, and the rate-determining step might be adsorption or activation of NO.²⁸ Similar to a Mn-based perovskite oxide, the NO conversion increases with an increase into the NO partial pressure. High NO conversion at low NO partial pressure is an important for a NO decomposition catalyst. However, at 1000 ppm NO, conversion of NO was still reasonably high (ca. 45%). Therefore, this SrFeO₃-based catalyst also exhibited high NO decomposition activity in a low P_{NO} range. N₂ formation rate is plotted against NO partial pressure in Fig. 6. The N₂ formation rate monotonically increased with an increase in the logarithm of NO partial pressure, and the P_{NO} dependence was $P_{\text{NO}}^{1.31}$, which is almost the same value with that of La(Ba)-Mn(In)O₃ in our previous study. This suggests that the adsorption and activation of NO are also important steps on Pt/SrFe_{0.7}Mg_{0.3}O₃ catalyst. Coupling of NO adsorption species

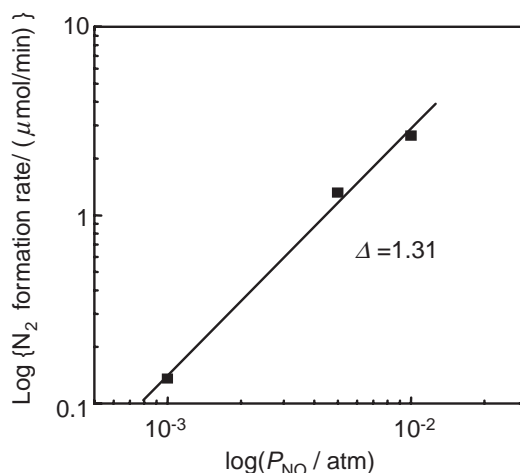


Fig. 6. N₂ formation rate from NO direct decomposition over 1 wt % Pt/SrFe_{0.7}Mg_{0.3}O₃ as a function of NO partial pressure at 1123 K ($W/F = 3.0 \text{ g s cm}^{-3}$).

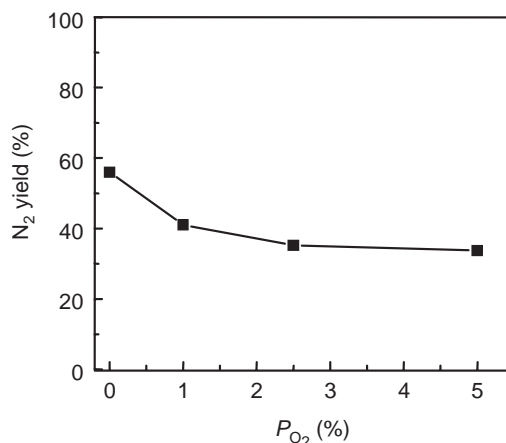


Fig. 7. N₂ yield from NO direct decomposition over 1 wt % Pt/SrFe_{0.7}Mg_{0.3}O₃ as a function of O₂ partial pressure at 1123 K ($P_{\text{NO}} = 0.5\%$, $W/F = 3.0 \text{ g s cm}^{-3}$).

is essentially required in some step for the formation of N₂ under NO decomposition, and for this, a high concentration of surface NO is needed.

Figure 7 shows the N₂ yield as a function of the O₂ partial pressure. In the conventional study, the presence of O₂ significantly lowered the catalyst activity for NO decomposition, and the number of the catalyst exhibiting a high NO conversion in the presence of O₂ was quite small. As shown in Fig. 7, the N₂ yield decreased from 56 to 42% in the presence of 1% O₂; however, the decrease in the N₂ yield was not significant in the P_{O_2} range from 1 to 5%. As a result, even under a P_{O_2} of 5%, a N₂ yield of 35% was obtained. Therefore, the negative effects of O₂ are not serious, and Pt-loaded SrFe_{0.7}Mg_{0.3}O₃ is highly tolerant against O₂. Figure 8 shows the N₂ formation rate as a function of oxygen partial pressure. The N₂ formation rate slightly decreased with an increase in the P_{O_2} , and the P_{O_2} dependency was as small as $P_{\text{O}_2}^{-0.12}$, which is much smaller than that of the similar perovskite oxides reported.²⁸ Therefore, the negative effects of O₂ are much smaller than that for other perovskite catalysts, and it is expected that a high

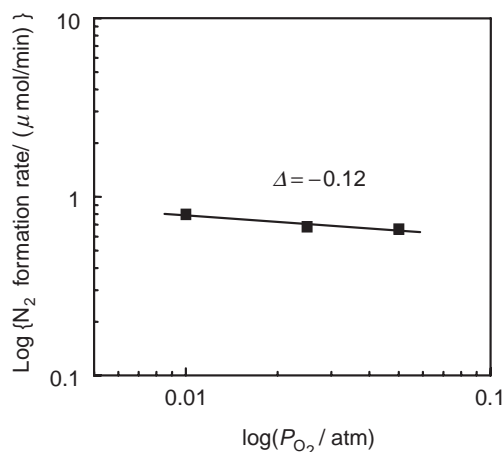


Fig. 8. N_2 formation rate from NO direct decomposition over 1 wt % Pt/SrFe_{0.7}Mg_{0.3}O₃ as a function of O_2 partial pressure at 1123 K ($P_{\text{NO}} = 0.5\%$, $W/F = 3.0 \text{ g s cm}^{-3}$).

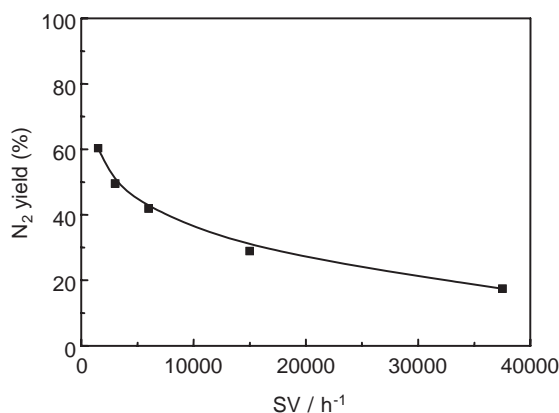


Fig. 9. N_2 yield from NO direct decomposition over 1 wt % Pt/SrFe_{0.7}Mg_{0.3}O₃ as a function of space velocity at 1123 K ($P_{\text{NO}} = 1.0\%$).

NO decomposition activity will be maintained for a longer period on this Pt-loaded SrFe_{0.7}Mg_{0.3}O₃ catalyst in the presence of O_2 .

In order to use a catalyst in an actual NO removal processes from automobile exhaust gas, a high NO removal rate should be maintained at a high space velocity. Since the NO decomposition reaction is considered a rather slow reaction, compared to the selective reduction of NO, the NO decomposition activity is generally lower at an elevated space velocity. In addition, BET surface area of perovskite oxide is small, that is, a few $\text{m}^2 \text{ g}^{-1}$, because high-temperature calcination is needed to obtain a single phase. In fact, the BET surface area of SrFeO₃-based oxide is less than $4 \text{ m}^2 \text{ g}^{-1}$ as shown in Table 1. Figure 9 shows the N_2 yield as a function of the space velocity of NO. N_2 formation rate decreased with an increase in the space velocity; however, a reasonably high N_2 formation rate was sustained at a high space velocity of NO, considering the BET surface area was about $1.7 \text{ m}^2 \text{ g}^{-1}$. In addition, a N_2 yield of 20% was still obtained at $\text{SV} = 40000 \text{ h}^{-1}$. Although the high activity is needed even at a few 100000 h^{-1} for a commercial de-NO_x catalyst, the NO decomposition activity of Pt-loaded SrFe_{0.7}Mg_{0.3}O₃ catalyst is reasonably high among

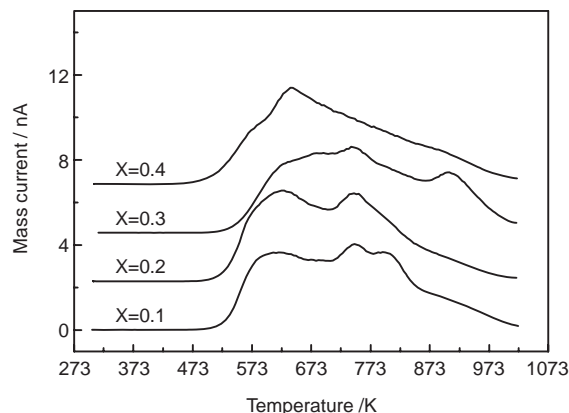


Fig. 10. O_2 desorption profiles from SrFe_{1-x}Mg_xO₃ (O_2 adsorption: 773 K for 1 h).

the conventional NO decomposition catalyst. Considering the BET surface area of the present catalyst, NO decomposition reaction at a large space velocity might be diffusion limited, and so, by increasing the surface area, it is thought that the NO decomposition activity should improve. Long-term stability of the NO decomposition activity over Pt-loaded SrFe_{0.7}Mg_{0.3}O₃ catalyst was also examined, and it was confirmed that the NO decomposition activity decreased negligibly up to 90 h after the reaction started. These results indicate that Pt-loaded SrFe_{0.7}Mg_{0.3}O₃ catalyst is active and good NO decomposition.

Effects of Mg Dopant and Pt Loading to O_2 and NO Adsorption State. Since the NO decomposition activity was greatly improved by doping Mg for Fe site and Pt loading, effects of the dopant and metal addition on NO and O_2 adsorptions were investigated by O_2 and NO-TPD. Normally, a higher NO decomposition activity tends to be achieved on a catalyst that weakly absorbs oxygen. In this study, change in oxygen adsorption state was investigated by O_2 -TPD.

Figure 10 shows the O_2 -TPD curves on SrFe_{1-x}Mg_xO₃. Oxygen desorption was observed at temperature higher than 523 K and desorption peaks at 573, 773, and 973 K, were observed on all catalysts. Comparing the desorption temperature of oxygen from the Mn-based perovskite oxide,²⁸ O_2 desorption temperature from SrFeO₃ is much lower, and the amount is also larger. This suggests that the strength of surface oxygen on SrFeO₃ is much weaker than that on LaMnO₃. The desorption temperature of oxygen around 573 K did not change with an increase in the Mg; however, the amount of total oxygen desorption increased with an increase in the Mg amount and reached a maximum at $x = 0.3$, at which the highest NO decomposition activity is achieved. Although quantitative analysis by mass spectrometry is not precise, it is noted that the peak area of TPD peaks from 323 to 1023 K was ca. 4% larger by addition of 30% Mg to Fe site of SrFeO₃. Therefore, the high NO decomposition activity on SrFe_{0.7}Mg_{0.3}O₃ can be explained by how easily the surface O_2 desorbs. The small P_{O_2} dependence of NO decomposition activity is also in good agreement with these results.

In contrast to oxygen desorption, NO desorption was not significantly affected by doping Mg for Fe site in SrFeO₃. Figure 11 shows the NO desorption curves from SrFe_{0.7}Mg_{0.3}O₃. As shown in Fig. 11, O_2 and N_2 formation was also

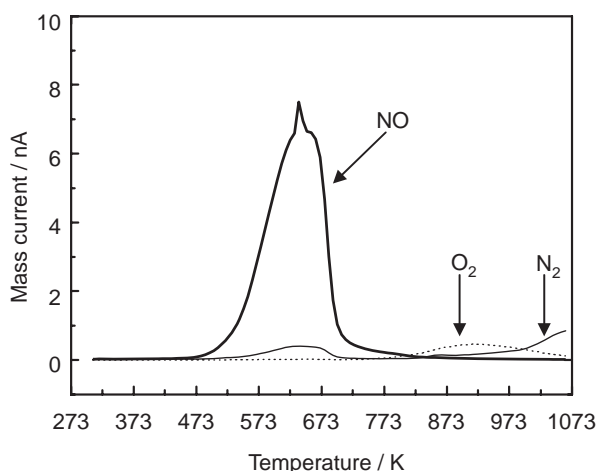


Fig. 11. NO desorption profiles from SrFe_{0.7}Mg_{0.3}O₃ (NO adsorption: 773 K for 1 h).

observed in NO-TPD. It was also observed that the molecular NO desorption occurred around 573 K, at which a fairly large amount of N₂ desorption was also observed. However, no oxygen desorbed at this temperature. This suggests that the formed oxygen was trapped on the surface of SrFeO₃-based oxide around 573 K. This trapped oxygen started to desorb above 773 K, followed by N₂ desorption. Therefore, it is thought that some amount of surface NO decomposed as the temperature increased and adsorption of NO is dissociative. Considering desorption of molecular NO and N₂ but not O₂, NO disproportionation reaction (for example; 3NO = N₂ + NO_{3ad}) occurs around 573 K, and the nitrogen oxide surface species may decompose at temperatures higher than 873 K. Therefore, desorption of O₂ and N₂ is observed at temperatures higher than 873 K. Formation of NO₃ surface species has also been observed on LaMnO₃ oxide.²⁸ This means that the surface of SrFe_{0.7}Mg_{0.3}O₃ is covered with oxygen formed by the decomposition of NO around 573 K. However, once the surface oxygen is removed, i.e., by decomposition of NO₃, NO direct decomposition seems to proceed, because N₂ desorption was observed after O₂ desorption was observed around 973 K. Therefore, SrFe_{0.7}Mg_{0.3}O₃ exhibits high activity toward NO direct decomposition at temperatures higher than 973 K due to desorption oxygen. If the adsorbed oxygen can be removed, then it can be expected that direct decomposition of NO will proceed at a temperature around 773 K. In any case, doping with Mg at the Fe sites of SrFeO₃ makes oxygen desorption easier.

Pt loading was also studied by O₂ and NO-TPD. Figure 12 shows the comparison of oxygen desorption profiles on SrFe_{0.7}Mg_{0.3}O₃ with and without Pt loading. Obviously, the desorption temperature of oxygen shifted to a lower temperature, and oxygen desorption was observed at temperatures as low as 473 K. In addition, large oxygen desorption peaks were also observed above 873 K, which were not observed on the catalyst without Pt. The total area of O₂-TPD peak on Pt loading one was 1.13 times larger than that of non Pt-loading catalyst. Therefore, it is clear that Pt loading is effective for decreasing oxygen desorption temperature and also enlarging the desorption amount. Since Pt is well-known reduction catalyst, small amount of surface Pt may work as the reduction

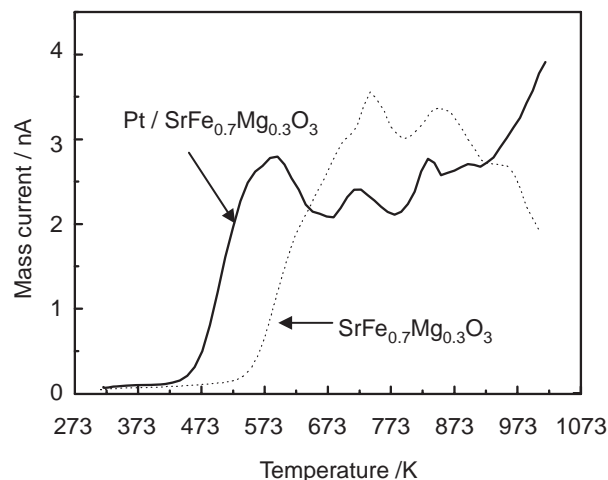


Fig. 12. O₂ desorption profiles from 1 wt % Pt/SrFe_{0.7}Mg_{0.3}O₃ and SrFe_{0.7}Mg_{0.3}O₃ (O₂ adsorption: 773 K for 1 h).

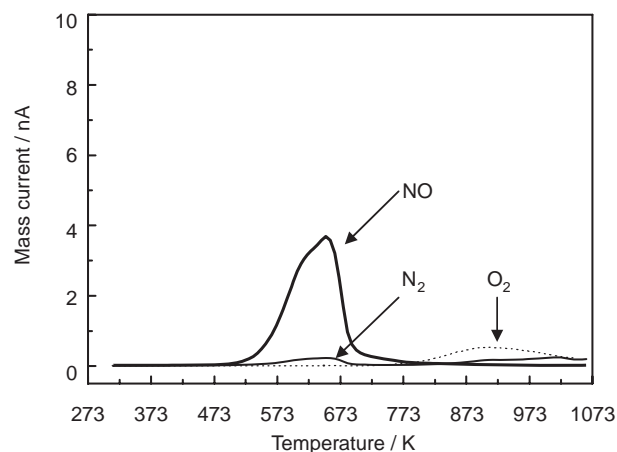


Fig. 13. NO desorption profiles from 1 wt % Pt/SrFe_{0.7}Mg_{0.3}O₃ (NO adsorption: 773 K for 1 h).

catalyst and is effective for removing the surface oxygen. This means that the surface Pt might be active to break the metal–oxygen bonds on the surface of SrFeO₃. Figure 13 shows the NO desorption profiles from Pt-loaded SrFe_{0.7}Mg_{0.3}O₃ catalyst. Similar to the profile for Mg doping, there were no significant changes in NO desorption profiles of Pt-loaded samples, except for a decrease in NO desorption amount and slight increase in oxygen desorption amount. Since the amount of desorbed N₂ and O₂ is slightly improved by loading Pt, the decrease in the amount of NO desorption (the peak area is almost half of non Pt-loaded one) suggests that Pt causes the NO dissociation on the surface and the amount of molecular NO adsorption decreases. However, amount of surface activated NO seems to increase with Pt loading. Therefore, it seems that the loaded Pt is effective for improving the surface active NO concentration. As discussed earlier, NO adsorption and activation seems to be important factors for NO decomposition activity on this catalyst, and so, Pt has a positive effect on the NO decomposition activity, because oxygen desorbs more readily and thus active sites are recovered.

NO adsorption state on Pt-loaded SrFe_{0.7}Mg_{0.3}O₃ catalyst

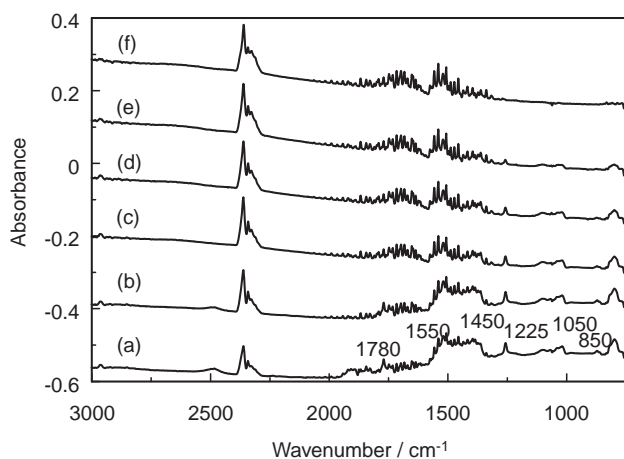


Fig. 14. IR spectra of adsorbed NO on 1 wt % Pt/SrFe_{0.7}Mg_{0.3}O₃: (a) NO adsorption at 773 K, (b) evacuation at room temperature, (c) evacuation at 473 K, (d) evacuation at 573 K, (e) evacuation at 673 K, (f) evacuation at 773 K.

was studied. Figure 14 shows the IR spectra of NO after adsorption at 773 K. After adsorption of NO at 773 K, absorption peaks at 1780, 1550, 1450, 1225, 1050, and 850 cm⁻¹ were observed. In comparison to the reported values,²⁸ the peak at 1780 and those around 1500 cm⁻¹ were assigned to bent-type NO (NO⁺) and nitrate oxides, such as NO₃ species. Therefore, adsorption of NO seems to be electron donative, i.e., the catalyst is reduced by adsorption of NO, and this is reasonable considering that Fe⁴⁺ is easily reduced to Fe³⁺, which is a more stable oxidation state. Since the absorption peak at 1780 cm⁻¹ disappeared after the sample was placed under a vacuum at 473 K for 30 min, the desorption peak of NO in NO-TPD around 623 K was assigned to that of bent-type NO adsorption species. On the other hand, absorption peaks around 1500 and 1000 cm⁻¹ remained after evacuation at 673 K, but disappeared after evacuation at 773 K evacuation, for 30 min. Therefore, O₂ and N₂ desorption peaks observed in NO-TPD at temperatures higher than 773 K were assigned to the decomposition products of nitrate species. Since nitrate species strongly cover the active sites for NO decomposition, removal of nitrate species from the surface is highly important to achieve high NO decomposition activity. Pt-loaded SrFe_{0.7}Mg_{0.3}O₃ catalyst needs a relatively low temperature for desorption of nitrate-like surface species resulting in the high NO decomposition activity in an intermediate temperature range. In any case, the decomposition of nitrate species, which forms by disproportionation of NO, is important step for NO decomposition reaction on SrFeO₃-based catalyst, and this seems to be accelerated by addition of small amount of Pt.

Conclusion

The NO decomposition activity increased in the order of Mg > Sn > Ni > Ce > Zr after doping the Fe site in SrFeO₃ perovskite oxide. Among the investigated dopants and compositions, the highest N₂ yield was achieved with SrFe_{0.7}Mg_{0.3}O₃. On this catalyst, NO conversion increased with an increase in the reaction temperature, and conversion of NO into N₂ and O₂ at 1123 K was 47 and 23%, respectively. The NO decomposition activity improved greatly by loading

a small amount of Pt. The N₂ yield increased from 47 to 56% and the light-off temperature of NO decomposition activity shifted by as much as 100 K to a lower temperature.

On Pt-loaded SrFe_{0.7}Mg_{0.3}O₃ catalyst, the NO decomposition rate increased with an increase in the NO partial pressure with $P_{\text{NO}}^{1.31}$. Therefore, the key step for NO decomposition on Pt-loaded SrFe_{0.7}Mg_{0.3}O₃ seems to be related with the adsorption or activation of NO. The presence of oxygen decreased the N₂ yield with $P_{\text{O}_2}^{-0.12}$; however, a N₂ yield of 35% was afforded even in the presence of 5% O₂ at 1123 K. Therefore, oxygen scarcely affects the decomposition reaction, and the effect of oxygen poisoning on NO decomposition upon Pt-loaded SrFe_{0.7}Mg_{0.3}O₃ is small. From the O₂-TPD results, Pt loading is thought to weaken the adsorption strength of the surface oxygen and to increase the decomposition of nitrate surface species. In summary, this study shows that substituting some of the Fe with a cation in a lower valence state in SrFeO₃ and also loading a small amount of Pt are highly effective for increasing the NO decomposition activity.

References

- 1 M. Iwamoto, *Shokubai* **1995**, 37, 614.
- 2 S. Kagawa, Y. Teraoka, *Hyomen* **1993**, 31, 913.
- 3 H. Hamada, *Shokubai* **1991**, 33, 320.
- 4 H. Hamada, Y. Kintaichi, M. Sasaki, T. Ito, M. Tabata, *Appl. Catal.* **1990**, 64, L1.
- 5 S. Sato, Y. Yu-u, H. Yahiro, N. Mizuno, M. Iwamoto, *Appl. Catal.* **1991**, 70, L1.
- 6 K. Yogo, M. Umeno, H. Watanabe, E. Kikuchi, *Chem. Lett.* **1993**, 131.
- 7 H. Hamada, Y. Kintaichi, M. Sasaki, T. Ito, T. Yoshinari, *Appl. Catal., A* **1992**, 88, L1.
- 8 M. Iwamoto, H. Yahiro, H. K. Shin, M. Watanabe, J. Guo, M. Konno, T. Chikahisa, T. Murayama, *Appl. Catal., B* **1994**, 5, L1.
- 9 K. Yogo, M. Ihara, I. Terasaki, E. Kikuchi, *Chem. Lett.* **1993**, 229.
- 10 Y. Li, J. N. Armor, *Appl. Catal., B* **1992**, 1, L31.
- 11 Y. Nishizaka, M. Misono, *Chem. Lett.* **1993**, 1295.
- 12 A. Obuchi, A. Ohi, M. Nakamura, A. Ogata, K. Mizuno, H. Ohuchi, *Appl. Catal., B* **1993**, 2, 71.
- 13 M. Inaba, Y. Kintaichi, H. Hamada, *Catal. Lett.* **1996**, 36, 223.
- 14 H. Iwakuni, A. Takami, K. Komatsu, *Science and Technology in Catalysis 1998, Proceedings of the Third Tokyo Conference on Advanced Catalytic Science and Technology*, **1999**, p. 251.
- 15 M. Iwamoto, H. Yahiro, S. Shundo, Y. Yu-u, N. Mizuno, *Appl. Catal.* **1991**, 69, L15.
- 16 W. Held, A. Koenig, T. Richter, L. Puppe, *SAE Tech. Pap. Ser.* 900496.
- 17 H. Hamada, N. Matsubayashi, H. Shimada, Y. Kintaichi, T. Ito, A. Nishijima, *Catal. Lett.* **1990**, 5, 189.
- 18 C. J. Bennett, P. S. Bennett, S. E. Golunski, J. W. Hayes, A. P. Walker, *Appl. Catal., A* **1992**, 86, L1.
- 19 K. Kharas, *Appl. Catal., B* **1993**, 2, 207.
- 20 H. Hamada, Y. Kintaichi, M. Sasaki, T. Ito, *Chem. Lett.* **1990**, 1069.
- 21 H. Yasuda, N. Mizuno, M. Misono, *J. Chem. Soc., Chem. Commun.* **1990**, 1094.

- 22 M. Iwamoto, H. Yahiro, K. Tanda, N. Mizuno, Y. Mine, S. Kagawa, *J. Phys. Chem.* **1991**, 95, 3727.
- 23 Y. F. Chang, J. G. McCarty, *J. Catal.* **1998**, 178, 408.
- 24 M. A. Vannice, A. B. Walters, X. J. Zhang, *J. Catal.* **1996**, 159, 119.
- 25 S. Xie, M. P. Rosynek, J. H. Lunsford, *J. Catal.* **1999**, 188, 24.
- 26 Y. Teraoka, H. Fukuda, S. Kagawa, *Chem. Lett.* **1990**, 1.
- 27 Y. Teraoka, T. Harada, S. Kagawa, *J. Chem. Soc., Faraday Trans.* **1998**, 94, 1887.
- 28 T. Ishihara, A. Ando, K. Takiishi, K. Yamada, H. Nishiguchi, Y. Takita, *J. Catal.* **2003**, 220, 104.
- 29 S. Shin, Y. Hatakeyama, K. Ogawa, K. Shimomura, *Mater. Res. Bull.* **1979**, 14, 133.
- 30 S. Shin, M. Yonemura, H. Ikawa, *Bull. Chem. Soc. Jpn.* **1979**, 52, 947.
- 31 S. Shin, M. Yonemura, H. Ikawa, *Mater. Res. Bull.* **1978**, 13, 1017.
- 32 S. Shin, H. Arakawa, Y. Hatakeyama, K. Ogawa, K. Shimomura, *Mater. Res. Bull.* **1979**, 14, 633.
- 33 R. D. Shannon, C. T. Prewitt, *Acta Crystallogr., Sect. B* **1969**, 25, 925; R. D. Shannon, *Acta Crystallogr., Sect. A* **1976**, 32, 751.
- 34 X. Wang, S. M. Sigmon, J. J. Spivey, H. H. Lamb, *Catal. Today* **2004**, 96, 11.
- 35 Z. Liu, J. A. Anderson, *J. Catal.* **2004**, 224, 18.